

Supplemental Information, Data, Figures & Tables (Zhang *et al.*)

Materials and Methods

Genotyping. DNA was extracted from a small piece of mouse ear tissue with sodium hydroxide and Tris (1), and the following primers (from 5' to 3') were used for genotyping:

Necab2 forward primer, ACCCAGACAACTCACTCATCAGAAGC;

Necab2 reverse primer, GGGGGTTCAGACTCAGCAATGT;

Common en2 reverse primer, CCAACTGACCTTGGGCAAGAACAT;

Common loxP forward, GAGATGGCGCAACGCAATTAAT.

Each sample needed two sets of primers for genotyping: *Necab2* forward and reverse primers, and the combination of all four primers. Samples from wild-type mice showed a single PCR product of 1.7 kb; samples from *Necab2*^{+/-} mice showed three PCR products of 1.7 kb, 400 base pairs (bp) and 300 bp; samples from *Necab2*^{-/-} mice showed two PCR products of 400 bp and 300 bp. Primers used for the genotyping of *Hoxb8-Flp* mice were:

Hoxb8 forward primer, CTCCCCAACAGCCCCCAACTACAG;

Flp reverse primer, GTCGCTGAACCTGCCGCAAGTTGATGAATGT.

Surgery. Complete transection of the sciatic nerve (axotomy) at mid-thigh level of the hind leg was performed as previously described (2). Briefly, mice were anesthetized with 1.5–1.8% (vol/vol) isoflurane (Baxter); the left sciatic nerve was transected at the mid-thigh level, and a 5-mm portion of the distal part was removed to prevent regeneration. Subsequently, the muscle and skin were closed with 5-0 silk sutures (Ethicon). Mice were allowed to survive for 3 d. SNI surgical procedures were performed under anesthesia with isoflurane as previously described (3, 4). Briefly, the skin of the mid-thigh from left lateral surface was incised, and a separation was made directly through the *biceps femoris* muscle exposing the three terminal branches of the sciatic nerve: common peroneal, tibial and sural nerves. The common peroneal and tibial nerves were tightly ligated with 6-0 silk (Ethicon), transected together distally to the ligation, and a piece of 1-2 mm of each nerve was removed from the distal stump. Any contact with or stretching of the intact sural nerve during the surgery process was avoided. Finally, muscle and skin were closed in two layers with 5-0 silk stitches. Mice were allowed to survive for 3 weeks. To induce peripheral inflammation, 20 µl of 1% λ carrageenan (Sigma) was injected into the intra-plantar part of the hind paw with a 28-G needle (5). Mice were allowed to survive for up to 1 week for behavior experiments; 45 min, 1.5h or 6h for gene expression analysis (for mRNA); 2h for Fos immunostaining and 3 days for immunohistochemical and biochemical experiments.

Quantitative real time-PCR (qPCR). Total RNA was isolated from mouse lumbar (L4-6) DRGs and corresponding spinal cord segments, homogenized by Motorized Pestle Mixer (Argos Technologies) using TRI Reagent (Sigma-Aldrich), and cDNA was generated from 500 ng RNA using High-Capacity cDNA Reverse Transcription Kit (Applied Biosystems) according to the manufacturer's instructions. qPCR reactions were performed using Maxima SYBR Green Master Mix with ROX (Thermo Scientific) on a QuantStudio5 System (Applied Biosystems). Primer pairs used in this study were listed in **Table**

S1. Amplification conditions were as follows: an initial stage at 50 °C for 2 min and 95 °C for 10 min, 40 cycles of 15 sec at 95 °C and 1 min at 60 °C. All assays were performed in duplicate and the levels of transcripts were analyzed by the comparative CT ($2^{-\Delta\Delta CT}$) method relative to *Gapdh*.

Western blotting. Proteins were extracted from freshly dissected DRGs and spinal cord from WT and *Necab2*^{-/-} mice using a radioimmunoprecipitation assay lysis buffer [50 mM Tris·HCl (pH 7.4), 1% Nonidet P-40, 0.25% sodium deoxycholate, 150 mM NaCl, and 1 mM EDTA] also containing a protease inhibitor mixture (P8340; Sigma). After sonication, lysates were centrifuged at 12,000g at 4 °C for 20 min. Supernatants were collected and the protein concentrations were determined by using the Bradford Protein Assay (Bio-Rad Laboratories). Laemmli sample buffer (1×, final) containing 20–30 µg of total protein lysate was loaded in each lane and separated on 10% SDS-PAGE gels, transferred onto PVDF membranes (Millipore), blocked with 5% non-fat dry milk in Tris-buffered saline with 0.1% Tween-20 (TBST) at 22–24 °C for 1h, and incubated with antibodies against NECAB1 (HPA023629) or NECAB2 (HPA014144 and HPA013998) (anti-rabbit, 1:1,000 in 5% BSA; Atlas Antibodies AB) at 4 °C overnight. Membranes were then incubated with HRP-conjugated secondary antibodies (1:5,000–1:10,000; DAKO) for at 22–24 °C for 1h, washed in TBST twice, exposed to ECL solution for 5 min (GE Healthcare), and scanned on a ChemiDOC⁺ Imaging system (Bio-Rad Laboratories). Membranes were stripped and re-probed with anti-GAPDH antibody (anti-mouse, 1:10,000 in 5% BSA; Ambion), which was used as loading control. Labeling intensities were quantified with Image Lab software (Bio-Rad Laboratories) on non-saturated images.

Tissues and immunohistochemistry. For immunohistochemistry, mice were deeply anesthetized with Na-pentobarbital (50 mg/kg, i.p.; APL) and perfused transcardially with 4% paraformaldehyde as previously described (6). Lumbar (L4 and L5) DRGs, corresponding lumbar segments of the spinal cord, sciatic nerve, and hind leg paws were dissected out and post-fixed in the same fixative for 90 min at 4 °C, followed by rinsing in 10% (vol/vol%) sucrose in 0.1M phosphate buffer containing 0.01% sodium azide (Merck) and 0.02% bacitracin (Sigma). Tissues were kept in 10% sucrose solution for 2 days at 4 °C. Tissues were trimmed and embedded with optimal cutting temperature compound (HistoLab AB), frozen in liquid carbon dioxide, and sectioned on a cryostat (Thermo) at a thickness of 12 µm for DRGs and 20 µm for spinal cords. Sections were mounted onto SuperFrost Plus microscope slides (VWR International) and stored at -20 °C. DRG sections were dried at 22–24 °C for at least 30 min and then incubated with a cocktail of primary antibodies (Table S2) diluted in PBS containing 0.2% (wt/vol) BSA (Sigma) and 0.3% Triton X-100 (Sigma) in a humid chamber at 4 °C for 18h. Non-commercial primary antibodies (Table S2) were donated by L. Terenius (Karolinska Institutet, Stockholm, Sweden) and I. Christensson (Uppsala University, Uppsala, Sweden) and M. Goldstein (New York University Medical Center, New York, NY, USA). Immunoreactivities were visualized using the TSA Plus kit (PerkinElmer) as previously described (6). For double labeling in DRGs, slides after TSA labeling were selected and rinsed in PBS for 20 min and then incubated with primary antibodies over 48 h at 4 °C. Slides were first washed in PBS for 30 min and then incubated with Cy3-conjugated, affinity-purified donkey anti-rabbit (or -mouse, -sheep, -goat) IgG (1:150; Jackson ImmunoResearch Laboratories) at 22–24 °C for 2h; after

rinsing, they were mounted in DABCO medium. For the staining of spinal cord from *Arc-Cre^{ERT2}/ZsGreen1* mice, primary antibodies were added alone or mixed together and incubated for 48h, followed by incubation of secondary antibodies conjugated to Cy3 or Cy5. Counterstaining by DAPI was performed as last step. Another set of DRG sections were incubated with IB4 from *Griffonia simplicifolia* I (GSA I) (2.5 g/mL; Vector Laboratories), followed by incubation with a goat anti-GSA I antiserum (1:1,000; Vector Laboratories) and incubation with Cy3-conjugated affinity-purified donkey anti-goat IgG at 22-24 °C for 2h to visualize IB4 binding.

Microscopy and image processing. Representative images were acquired on an LSM700 confocal laser-scanning microscope (Carl Zeiss) equipped with an EC Plan-Neofluar objective with a magnification of 10x and N.A. of 0.30 and a water-immersion objective with a magnification of 40x and N.A. of 1.40. (pinhole set to one airy unit throughout). Emission spectra for each dye were limited as follows: DAPI (<480 nm), FITC/Alexa Fluro488/Cy2 (505-540 nm), Cy3/PI (560-610 nm) and Cy5 (>650 nm). For projection images, orthogonal z-stacks were acquired with a step interval of 1 μm at a primary magnification of 40x. Images were processed in ZEN2012 software (Zeiss). Multi-panel figures were assembled using Adobe Photoshop CS6 software (Adobe Systems).

Quantitative morphometry. For quantification of neuronal profiles (NPs) in DRGs, 3-5 L5 DRG sections were selected from different levels (at a 1:4 interval), immunostained for NECAB2 or BDNF (peripheral nerve injury or inflammatory models) and counterstained with 0.001% propidium iodide (PI; Sigma). Sections were tile-scanned with an LSM700 laser-scanning microscope equipped with a Plan-Apochromat M27 objective (20x and N.A. of 0.80). NPs with intensity of NECAB2- or BDNF-like immunoreactivity (LI) higher than mean \pm 2x S.D. of the background were considered positive. The total number of DRG NPs was counted on PI-stained DRGs. All of the counting, including the quantification of co-localization (~3 sections/marker), was performed using Adobe Photoshop CS6. The cross-sectional area and intensity (mean gray value) were also determined in ImageJ v.1.46 (National Institutes of Health). Size distribution was plotted as described by Scherrer *et al.* using a size cut-off classification criteria as follows: small (<300 μm^2), medium (300-700 μm^2) and large (>700 μm^2) (7). To determine fluorescence intensity in spinal cord, sections were tile-scanned with an LSM700 laser-scanning microscope equipped with an EC Plan-Neofluar objective at a primary magnification of 10x. Fluorescence intensity (mean gray value) from different spinal dorsal horn layers was read out with ImageJ v.1.46.

iDISCO⁺ method and volume imaging. iDISCO⁺ volume immunostaining and tissue clearing were performed as described (8). Briefly, blocks of spinal cord were washed in 0.01 M PBS (3x in 5 ml Eppendorf tubes) and dehydrated in an ascending series of methanol/water (1h each). Samples were bleached with 5% hydrogen peroxide in 100% methanol overnight at 4 °C. Subsequently, specimens were rehydrated, incubated in permeabilization solution for 2 days followed by blocking for another 2 days, both at 37 °C (in 0.2% Triton-X100, 20% DMSO, 0.3M glycine in 0.01M PBS supplemented by 0.02% sodium azide and 0.2% Triton-X100, 10% DMSO, 6% normal donkey serum in 0.01 M PBS to

which 0.02% sodium azide had been added, respectively). Samples were then incubated with primary antibody (anti-NECAB2, rabbit polyclonal (HPA014144), 1:200) for 4 days at 37 °C (diluent: 0.2% Tween-20, 10 µg/ml heparin, 5% DMSO, 3% normal donkey serum, 0.02% Na-azide in 0.01 M PBS). After extensive washing, tissue blocks were incubated in Alexa Fluor 647-conjugated goat anti-rabbit secondary antibody (1:200, Molecular Probes) in 0.2% Tween-20, 10 µg/ml heparin, 3% normal donkey serum, 0.02% Na-azide in 0.01M PBS. Blocks were next dehydrated in an ascending series of methanol and water, incubated in a mixture of 66% dichloromethane and 33% methanol for 3h, and in 100% dichloromethane for 2 x 15 min. Finally, imaging-ready tissue blocks were transferred into tubes filled with 100% dibenzyl ether for long-term storage. For imaging, a light-sheet microscope (Ultramicroscope II, Lavisision Biotec) was used with the following parameters: laser power: 72%; exposure time: 100 ms; light-sheet N.A.: 0.056; magnification: 3.2x; step size: 2 µm; 25-step dynamic focus with 'contrast filtered' merging algorithm. Altogether, 5.2 mm and 2 mm-long samples (medulla-cervical spinal cord and lumbar spinal cord, respectively) were acquired. Serial images were converted into an IMS file, and three-dimensionally reconstructed in Imaris™ 8.4.0 (Bitplane). Brightness/contrast adjustment, gamma correction and background subtraction were occasionally applied to improve image quality.

Supporting Results

Characterization of anti-NECAB2 antibodies. *Necab2*^{-/-} mice were generated by using the promoter-driven knockout first strategy (Figure 3A) (9). The NECAB2 antibody (HPA013998) used in our previous study (10) showed staining in DRGs but not spinal cord from *Necab2*^{-/-} mice (Figure 3A). A second anti-NECAB2 antibody (HPA014144) raised against its C-terminal did not show any off-target staining in either DRGs or spinal cord (Figure 1A,B,L,M and 3C) and henceforth used throughout. The difference in staining in DRGs could be caused either by a residual (truncated) NECAB2 fragment in *Necab2*^{-/-} mice encoded by its exons 1-3 (Figure 3A,C) or by cross-reactivity to NECAB1. The latter assumption is in view of the high similarity between the human NECAB2 PrEST used for immunization and mouse NECAB1 (68%, Figure 3C). We advocate the latter option since the HPA103998 antibody did not show any NECAB2 staining in the spinal cord of *Necab2*^{-/-} mice. Therefore, NECAB2 expression in ~70% of all DRG neuron profiles (NPs) reported in our previous study is an overestimate, likely caused by cross-reactivity with NECAB1. We propose this explanation even if both antibodies show bands at the calculated molecular weight of NECAB2 in Western blotting (Figure 3D). Nevertheless, our prior overestimate (10) does not change the fact that axotomy decreases NECAB2 immunoreactivity in DRG (originally from 74% to 54%), since our present data (from 34% to 13%) recapitulate earlier observations. These observations highlight that an antibody may show correct staining in one tissue but not another, and underlie the importance of testing antibody specificity for each tissue/organ/system analyzed in knock-out mice (11, 12).

Characterization of anti-secretagogin antibodies. In a previous study, we reported that the Ca²⁺-binding protein secretagogin is expressed in DRG neurons, as well as fibers in lamina I and in a specific population of interneurons in the mid-layer of lamina II. These interneurons overlapping with IB4 staining (6). Since then, we have generated *Scgn*^{-/-} mice, and used those to quality-control the immunoeagents available to us. Here, we confirm that secretagogin immunoreactivity of DRG neurons and motor neurons is absent in *Scgn*^{-/-} mouse. However, faint immunoreactivity in spinal lamina II persists in both *Scgn*^{-/-} and wild-type mice (*data not shown*). Therefore, we can formulate that secretagogin is expressed in a subpopulation of peptidergic DRG neurons projecting to lamina I of the spinal cord, some scattered interneurons and also in motor neurons, but not in unidentified structures of lamina II.

Supporting Figures & Legends

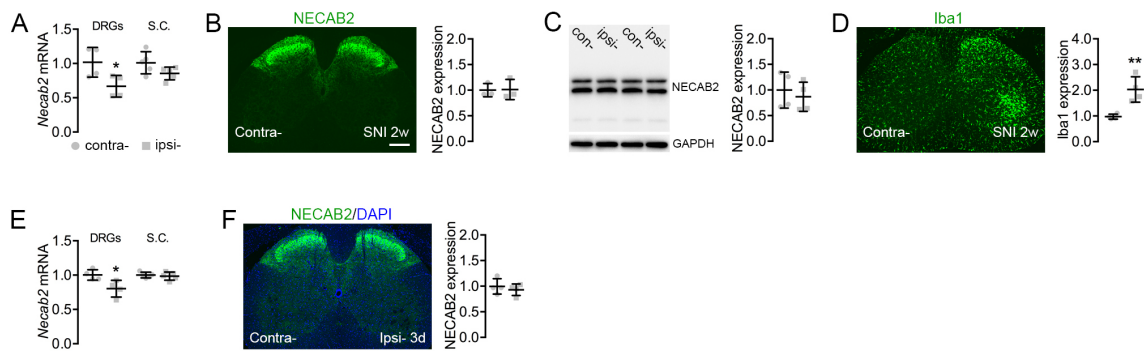


Figure S1. NECAB2 expression in mouse spinal cord. **A.** *Necab2* mRNA in DRGs and spinal cord (S.C.) 2 weeks after spared nerve injury (SNI; $n = 5$ /group). **B,C.** Effect of SNI (2-week survival) on the expression of NECAB2 in spinal cord; analysis by immunohistochemistry (B) and Western blotting (C). **D.** Activation of Iba1⁺ microglia in the dorsal and ventral spinal horn after SNI. **E.** *Necab2* mRNA in DRGs and spinal cord (S.C.) 3d after the onset of inflammation ($n = 5$ /group). **F.** Expression of NECAB2 in spinal cord (counterstained with DAPI) after 3 days of inflammation. Data were expressed as means \pm S.D. * $p < 0.05$, ** $p < 0.01$; Student's *t*-test. Scale bars = 200 μ m (B,D,F).

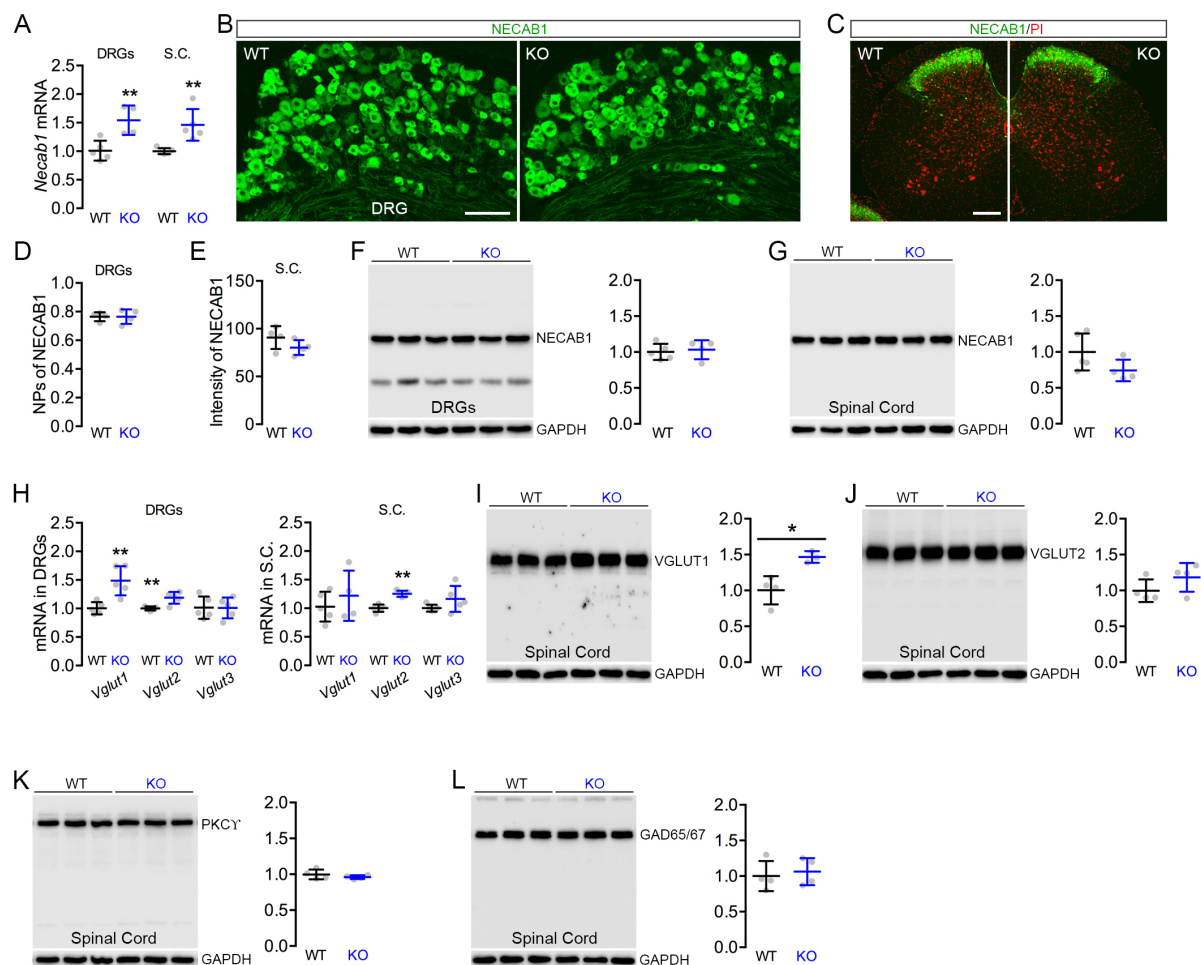


Figure S2. Biochemical survey of spinal cord in *Necab2*^{-/-} DRGs and spinal cord. **A.** Quantification of *Necab1* mRNA in DRGs and spinal cord from wild-type (WT) and *Necab2*^{-/-} mice ($n = 5$ in each group) analyzed with qPCR. **B,C.** Distribution of NECAB1 in DRGs (B) and spinal cord (C) from WT and *Necab2*^{-/-} mice. Red label in (C) is for propidium-iodide nuclear counterstaining. **D,E.** Quantification of NECAB1⁺ NPs in DRGs and relative intensity of NECAB1 immunoreactivity in spinal dorsal horn ($n = 4$ /group). **F,G.** Quantification of NECAB1 expression by Western blotting in DRGs and spinal cord from WT ($n = 5$) and *Necab2*^{-/-} mice ($n = 4$). **H.** Quantification of *Vglut1-3* mRNAs in DRGs and spinal cord from WT and *Necab2*^{-/-} mice ($n = 5$ /group) by qPCR. **I,J.** Quantification of VGLUT1 and VGLUT2 protein content in spinal cord by Western blotting ($n = 3-5$ /group). **K.** Analysis of PKCγ levels in spinal cord from WT and *Necab2*^{-/-} mice by Western blotting ($n = 4$ /group). **L.** Quantification of GAD65/67 levels in spinal cord from WT and *Necab2*^{-/-} mice ($n = 4$ /group). Data were expressed as means \pm S.D. * $p < 0.05$, ** $p < 0.01$. Scale bars = 100 μ m (B), 200 μ m (C).

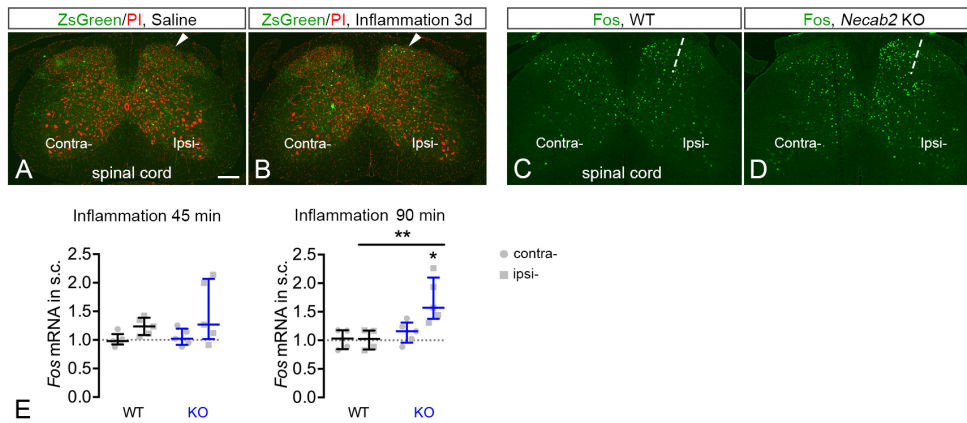


Figure S3. Trans-synaptic activation of *Arc* and *Fos* in spinal cord. **A,B.** Overview of the selective accumulation of *ZsGreen1* in spinal superficial layers counterstained with propidium iodide during the first 3 days of inflammation. Arrowheads indicate the area of selective *ZsGreen1* expression not seen after saline administration. **C,D.** Overview of *Fos* activation in spinal cord 2h after the induction of inflammation from WT and *Necab2*^{-/-} mice, especially ipsilaterally and medial to the dashed line. **E.** Gradual induction of *Fos* mRNA in spinal cord of *Necab2*^{-/-} but not wild-type mice 45 min and 90 min after the induction of inflammation ($n = 5/\text{group}$). Two-way ANOVA revealed a significant inflammation \times genotype interaction [$F_{(1, 14)} = 5.277, p = 0.0375$] with Bonferroni *post-hoc* test returning $*p < 0.05, **p < 0.01$ when comparing independent groups. Scale bars = 200 μm (A-D).

Supplemental Tables

Table S1. Primers for real-time PCR

Gene	Primer sequences (5'-3')
<i>Bdnf</i>	Forward: GATGCCGCAAACATGTCTATGA Reverse: TAATACTGTCACACACGCTCAGCTC
<i>Fos</i>	Forward: ATCCTTGGAGCCAGTCAAGA Reverse: ATGATGCCGGAACAAGAAG
<i>Il1b</i>	Forward: GAATCTATACCTGTCCTGTG Reverse: TTATGTCCTGACCACTGTTG
<i>Il6</i>	Forward: CTCATTCTGCTCTGGAGCCC Reverse: TGCCATTGCACAACCTTTTTCT
<i>Necab1</i>	Forward: CCACCTCCAGACGAATTACA Reverse: CCATGAAGCAGGAAGTAGCA
<i>Necab2</i>	Forward: CGACAGGACCACTGCAAA Reverse: CACAGGCAGGCTTTCATC
<i>Vglut1</i>	Forward: TTCTGGTTGCTTGTCTCC Reverse: CAGGGTGTGTTAACTTC
<i>Vglut2</i>	Forward: GGCAGTATGTCTTCCTCATTG Reverse: TTCTTCATCCAGTTCATCTTCG
<i>Vglut3</i>	Forward: TCATCTTCTACGGGGTCTTCG Reverse: CTCCTCAGCTAACTCATCTTGG
<i>Tnfa</i>	Forward: GACCCTCACACTCAGATCATCT Reverse: CCTCCAATTGGTGGTTTGCT
<i>Gapdh</i>	Forward: AACTTTGGCATTGTGGAAGG Reverse: ACACATTGGGGGTAGGAACA

Table S2. Primary antibodies used for this study

Antibody	Host	Supplier/Catalog number	Dilution
BDNF	Rabbit /polyclonal	Amgen Inc	1:2,000
calbindin-D28k	Rabbit /polyclonal	Swant /CB 38	1:400 (normal)
Fos	Rabbit /polyclonal	Calbiochem /PC38	1:2,000
CGRP	Rabbit /polyclonal	Terenius L. (Stockholm) and Christensson I. (Uppsala)	1:20,000 (normal)
Iba1	Rabbit /polyclonal	WAKO /019-19741	1.4,000
NECAB1	Rabbit /polyclonal	Atlas Antibodies AB /HPA023629	1:1,000
NECAB2	Rabbit /polyclonal	Atlas Antibodies AB /HPA014144	1:1,000
NF200	Mouse /monoclonal	Sigma /N0142	1:500 (normal)
PKC γ	Rabbit /polyclonal	Santa Cruz /sc-211	1:2,000
secretagoin	Rabbit /polyclonal	Atlas Antibodies AB /HPA006641	1:2,000
VGLUT1	Goat /polyclonal	Watanabe M. (Sapporo, Japan)	1:300 (normal)
VGLUT2	Guinea pig /polyclonal	Watanabe M. (Sapporo, Japan)	1:500 (normal)
TH	Rabbit /polyclonal	Goldstein M. (New York)	1:4,000
TrkB	Goat /polyclonal	R&D systems	1:1,000 (normal)

References

1. Truett GE, Heeger P, Mynatt RL, Truett AA, Walker JA, and Warman ML. Preparation of PCR-quality mouse genomic DNA with hot sodium hydroxide and tris (HotSHOT). *Biotechniques*. 2000;29(1):52, 4.
2. Wall PD, Devor M, Inbal R, Scadding JW, Schonfeld D, Seltzer Z, et al. Autotomy following peripheral nerve lesions: experimental anaesthesia dolorosa. *Pain*. 1979;7(2):103-111.
3. Decosterd I, and Woolf CJ. Spared nerve injury: an animal model of persistent peripheral neuropathic pain. *Pain*. 2000;87(2):149-158.
4. Pertin M, Gosselin RD, and Decosterd I. The spared nerve injury model of neuropathic pain. *Meth Mol Biol*. 2012;851:205-112.
5. Morris CJ. Carrageenan-induced paw edema in the rat and mouse. *Meth Mol Biol*. 2003;225:115-121.
6. Shi TJ, Xiang Q, Zhang MD, Tortoriello G, Hammarberg H, Mulder J, et al. Secretagoin is expressed in sensory CGRP neurons and in spinal cord of mouse and complements other calcium-binding proteins, with a note on rat and human. *Mol Pain*. 2012;8:80.
7. Scherrer G, Low SA, Wang X, Zhang J, Yamanaka H, Urban R, et al. VGLUT2 expression in primary afferent neurons is essential for normal acute pain and injury-induced heat hypersensitivity. *Proc Natl Acad Sci USA*. 2010;107(51):22296-22301.
8. Renier N, Adams EL, Kirst C, Wu Z, Azevedo R, Kohl J, et al. Mapping of Brain Activity by Automated Volume Analysis of Immediate Early Genes. *Cell*. 2016;165(7):1789-1802.
9. Skarnes WC, Rosen B, West AP, Koutsourakis M, Bushell W, Iyer V, et al. A conditional knockout resource for the genome-wide study of mouse gene function. *Nature*. 2011;474(7351):337-342.
10. Zhang MD, Tortoriello G, Hsueh B, Tomer R, Ye L, Mitsios N, et al. Neuronal calcium-binding proteins 1/2 localize to dorsal root ganglia and excitatory spinal neurons and are regulated by nerve injury. *Proc Natl Acad Sci USA*. 2014;111(12):E1149-1158.
11. Uhlen M, Bandrowski A, Carr S, Edwards A, Ellenberg J, Lundberg E, et al. A proposal for validation of antibodies. *Nat Methods*. 2016;13(10):823-827.
12. Saper CB. An open letter to our readers on the use of antibodies. *J Comp Neurol*. 2005;493(4):477-478.

Supplemental Figures of Uncut Gels (Zhang *et al.*)

Gels (all targets are shown on uncut gels; Figures 3 and S1,2 were included in this file)

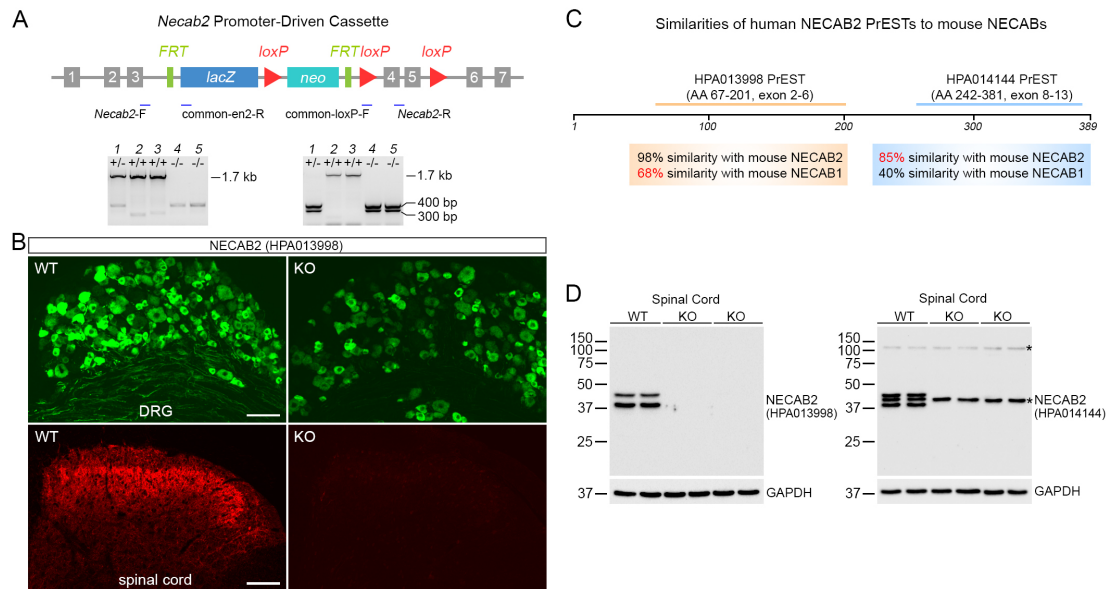


Figure 3. Generation of *Necab2*^{-/-} mice and antibody validation. **A.** Construct for knockout-first, promoter-driven *Necab2*^{-/-} [*Necab2* (tm1a)] mice. Primers (blue lines indicate locations) used for genotyping are shown together with PCR products from wild-type (lanes 2 and 3), heterozygous (lane 1) and *Necab2*^{-/-} offspring (lanes 4 and 5). **B.** Staining pattern of previously used anti-NECAB2 antibody (HPA013998) in DRGs (green) and spinal cord (red) of wild-type (WT) and *Necab2*^{-/-} mice. **C.** Comparison of human NECAB2 protein epitope signature tags (PrESTs) with mouse NECAB1 and NECAB2. **D.** Western blotting of NECAB2 with spinal cord lysates from WT and *Necab2*^{-/-} mice using HPA013998 and HPA014144 anti-NECAB2 antibodies. Note that antibody HPA014144 has an unspecific band (asterisk) between two specific bands. Representative data from $n = 2$ wild-type and $n = 4$ *Necab2*^{-/-} mice are shown. Another non-specific band occurs above 100 kDa, also indicated with asterisk. Scale bar = 100 μ m (B).

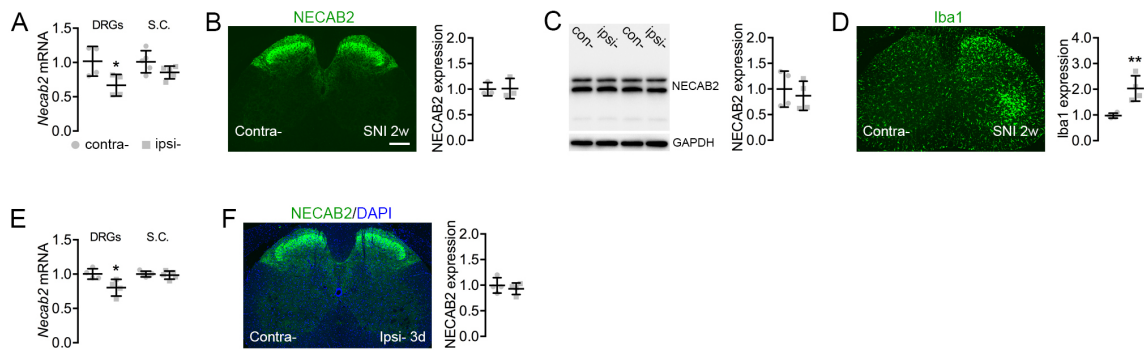


Figure S1. NECAB2 expression in mouse spinal cord. **A.** *Necab2* mRNA in DRGs and spinal cord (S.C.) 2 weeks after spared nerve injury (SNI; $n = 5/\text{group}$). **B,C.** Effect of SNI (2-week survival) on the expression of NECAB2 in spinal cord; analysis by immunohistochemistry (B) and Western blotting (C). **D.** Activation of Iba1⁺ microglia in the dorsal and ventral spinal horn after SNI. **E.** *Necab2* mRNA in DRGs and spinal cord (S.C.) 3d after the onset of inflammation ($n = 5/\text{group}$). **F.** Expression of NECAB2 in spinal cord (counterstained with DAPI) after 3 days of inflammation. Data were expressed as means \pm S.D. * $p < 0.05$, ** $p < 0.01$; Student's *t*-test. Scale bars = 200 μm (B,D,F).

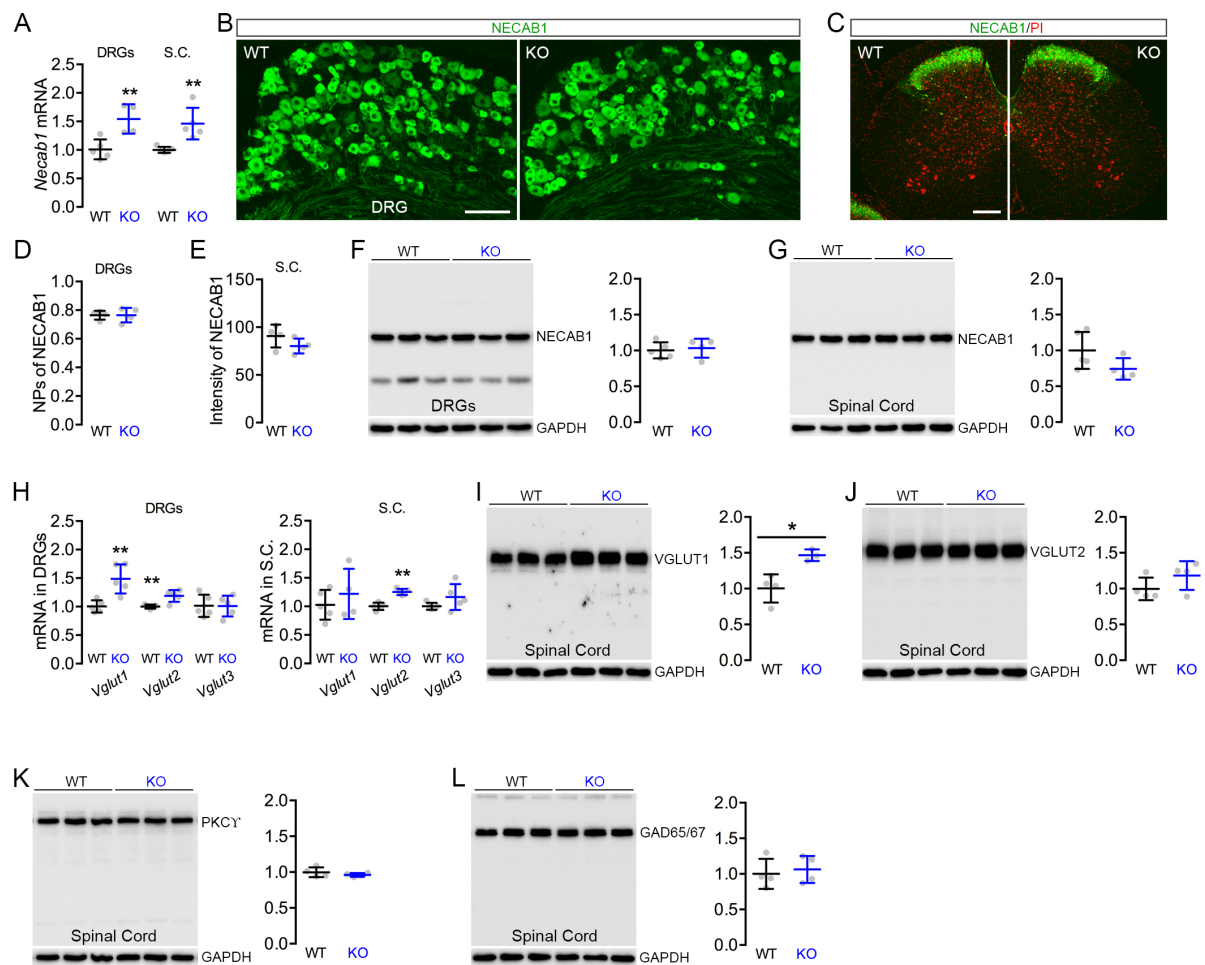
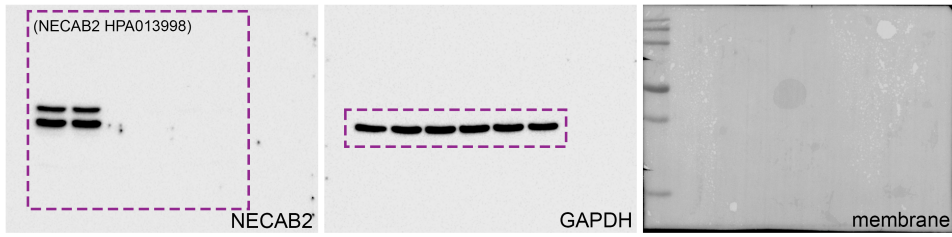


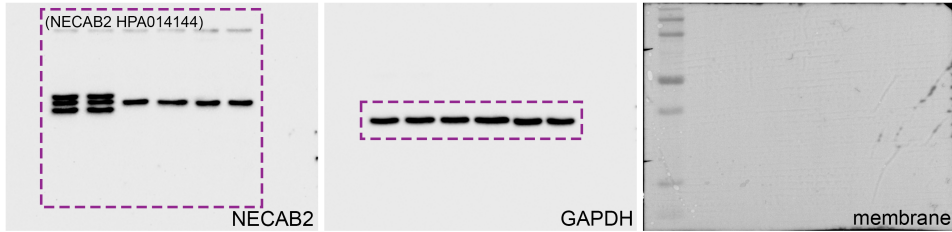
Figure S2. Biochemical survey of spinal cord in *Necab2*^{-/-} DRGs and spinal cord. **A**, Quantification of *Necab1* mRNA in DRGs and spinal cord from wild-type (WT) and *Necab2*^{-/-} mice ($n = 5$ in each group) analyzed with qPCR. **B,C**, Distribution of NECAB1 in DRGs (B) and spinal cord (C) from WT and *Necab2*^{-/-} mice. Red label in (C) is for propidium-iodide nuclear counterstaining. **D,E**, Quantification of NECAB1⁺ NPs in DRGs and relative intensity of NECAB1 immunoreactivity in spinal dorsal horn ($n = 4$ /group). **F,G**, Quantification of NECAB1 expression by Western blotting in DRGs and spinal cord from WT ($n = 5$) and *Necab2*^{-/-} mice ($n = 4$). **H**, Quantification of *Vglut1-3* mRNAs in DRGs and spinal cord from WT and *Necab2*^{-/-} mice ($n = 5$ /group) by qPCR. **I,J**, Quantification of VGLUT1 and VGLUT2 protein content in spinal cord by Western blotting ($n = 3-5$ /group). **K**, Analysis of PKC γ levels in spinal cord from WT and *Necab2*^{-/-} mice by Western blotting ($n = 4$ /group). **L**, Quantification of GAD65/67 levels in spinal cord from WT and *Necab2*^{-/-} mice ($n = 4$ /group). Data were expressed as means \pm S.D. * $p < 0.05$, ** $p < 0.01$. Scale bars = 100 μ m (B), 200 μ m (C).

Uncut gels (with figure panels in which they appear indicated)

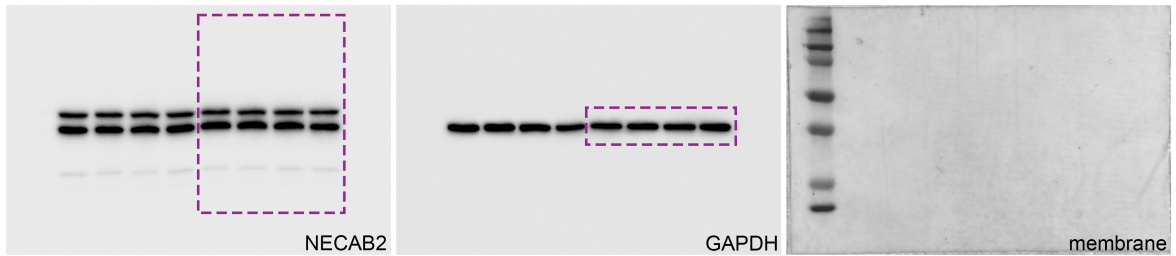
Full unedited gel for Figure 3D, left panel



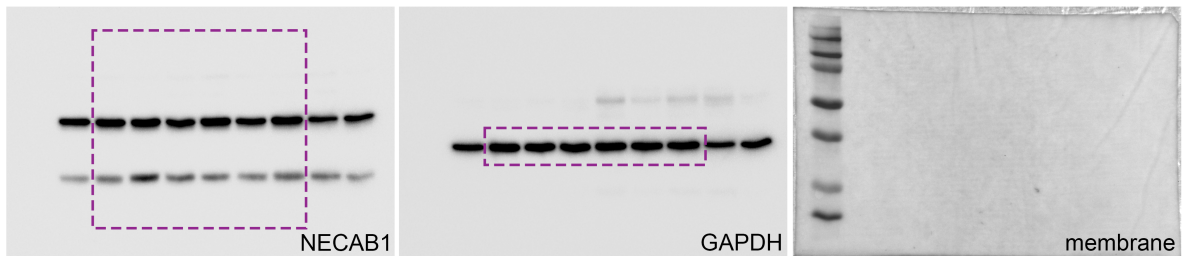
Full unedited gel for Figure 3D, right panel



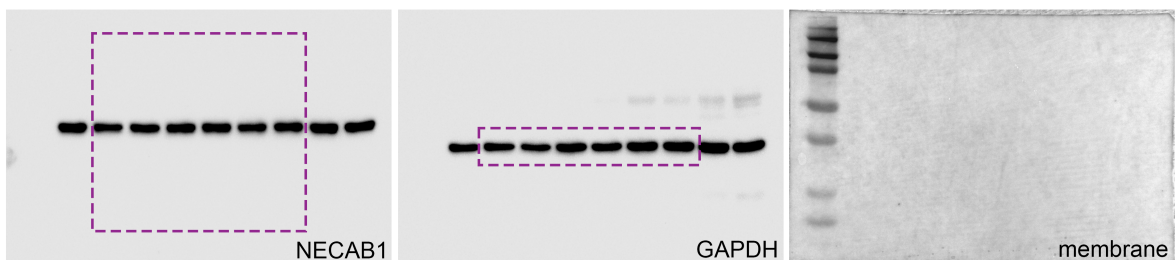
Full unedited gel for Figure S1C



Full unedited gel for Figure S2F

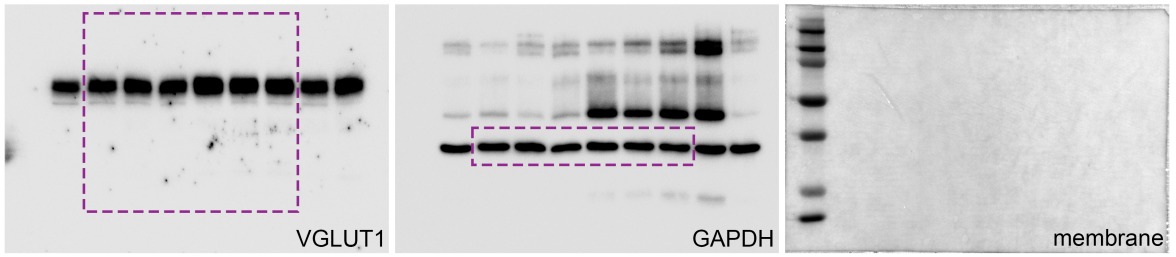


Full unedited gel for Figure S2G

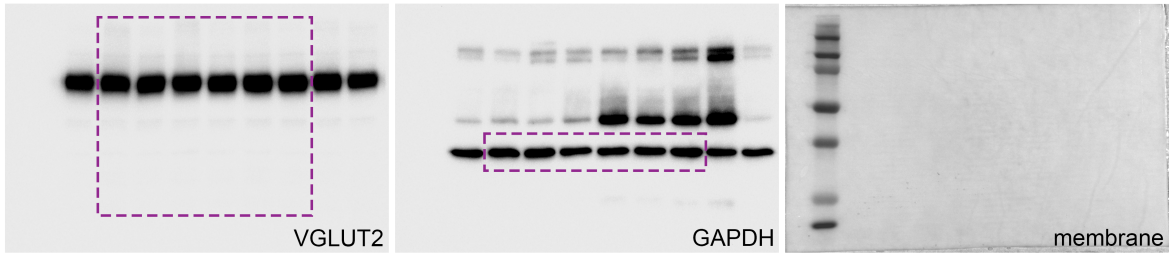


Uncut gels (with figure panels in which they appear indicated), continued:

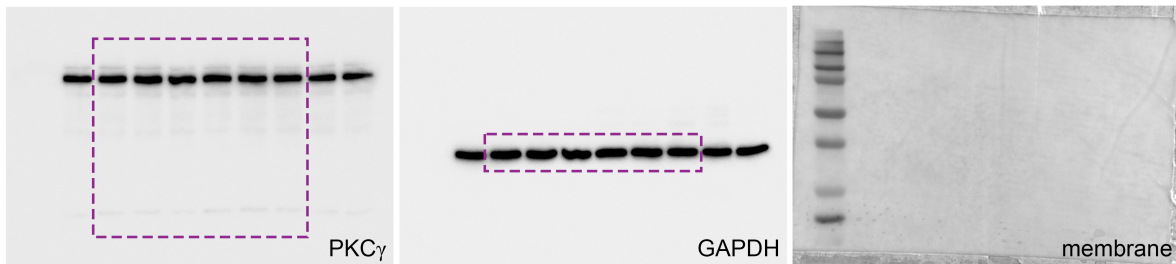
Full unedited gel for Figure S2I



Full unedited gel for Figure S2J



Full unedited gel for Figure S2K



Full unedited gel for Figure S2L

